Condition of the Sangdong Tungsten Skarn Formation

Kun Joo Moon*

Abstract: Fluid inclusion and stable isotope studies on the Sangdong tungsten skarn have led to a conclusion that the mineralizing fluids might be derived from a magma, which was inferred within 1km below the present Sangdong ore deposit.

Mineral assemblages of the skarns appear to have formed under the equilibrium conditions as the fluids flow outward from a central fluid column, in which the quatz-mica occurs dominantly.

A characteristic skarn showing mineralogical zonation by repeated over-prints.

The quartz-mica zone at the central part of the Sangdong skarns shows the final stage of pro-tracted fluid evolution.

Thermodynamic conclusion based on simplified chemical compositions of major components may express quantitatively the conditions of the skarn formation by using diagrams.

INTRODUCTION

The Sangdong tungsten skarns are products of metasomatic replacement of the interbedded limestones in the Myobong Slate and the lower parts of the Pungchon Limestone Series of Cambro-Ordovician age. The skarns show zonal distribution of the major skarn minerals (Fig. 1). A central quartz-mica zone is surrounded by an amphibole-rich zone which is enveloped by a pyroxene-garnet zone having abrupt outer contacts with unaltered Cambrian limestone.

$\delta^{18}O$ values in skarn quartz(+10.8 permil) $\delta^{34}S$ in skarn sulphide(+3.9 to +6.1 permil) and $\delta^{13}C$ and $\delta^{18}O$ in skarn carbonate (-8.1 and +11.8 permil respectively) indicate deri-vation from magmatic fluids, and the high tem-peratures indicated by the mineralogy and fluid inclusions(up to 600°C) suggest a magmatic heat source(Moon, 1983). Based on these results a possible existence of igneous pluton as a source rock was inferred. Recent drilling has confirmed the successful approach by intersecting altered granite within Precambrian rocks over 500 meter below the skarns.

* Korea Institute of Energy and Resources (KIER)

The skarn assemblages at Sangdong are broa-dly similar to those in other tungsten deposits (e.g. King Island in Australia, Salau in France, Pine Creek in U.S.A., MacTung in Canada). However, in detail there are important differ-ences, Particularly in mineral proportions, e.g. some of the Sangdong samples are almost mono-mineralic. As in other skarns (see, for example, Kwak, 1978a, b: Guy, 1979: Newberry, 1982: Dick and Hodgson, 1982), there is clear over-printing, indicating a protracted fluid evolution, perhaps with changing fiuid composition and temperature. The major mineralogical zoning pattern: (Fig. 1) mica - amphibole - pyroxene, results from intergranular fluid flow outward from a central fluid column. Though diffusion must have taken place, the scale of the zones demands "infiltration metasomatism" (Korzhinski, 1968, 1970) as the dominant mechanism. As the hydrous skarns migrate from the feeder column, earlier pyroxene-garnet $\pm$ wollastonite skarn is replaced successively by late stage pyro-xene-garnet, and then amphibole-and mica-rich assemblages. Petrographic evidence indicates that the amphibole-and mica-rich zones migrate toge-ther, more or less at "equilibrium", and with only minor relics of earlier assemblages within
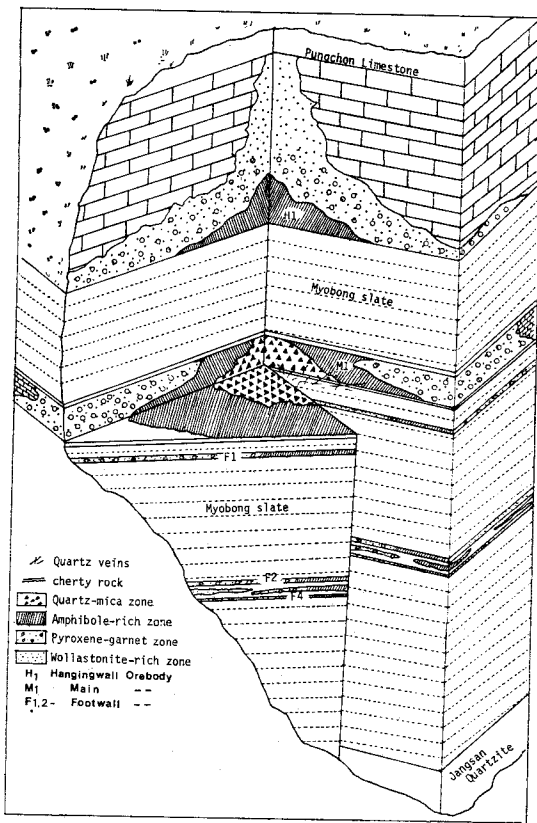
Fig. 1 A schematic view of the zonation in skarn orebodies.

them. However, the amphibole "front" against the late pyroxene-garnet zone is clearly one of replacement and the pyroxene-garnet zone itself is in process of patchy recrystallization with growth of secondary garnets and pyroxenes and localized alteration to amphibole. The dramatic chemical changes and the tendency for metasomatic rocks to become almost monomineralic (e.g. hedenbergite in the late pyroxene garnet skarn) further supports infiltration processes and an abundance of "mobile" components (Rose and Burt, 1976)

The system was "open" in a chemical sense and resulted from interaction between waves of hot fluid and original or metamorphosed rock. Though the fluids penetrating the lower part of the mine succession were initially largely of

magmatic origin, secondary circulation of these fluids as they became modified by rock interaction and the likely incorporation of ground water, probably resulted in the presence of fluids of complex origin(Moon, 1983).

In this paper, evaluation is made of the P–T–X conditions responsible for some of the major assemblages. All the thermodynamic data were obtained from Robie et al(1978), and Helgeson (1969) or calculated from data in Helgeson et al (1978). and Barin et al (1977). Some general trends in condition and composition are shown in Fig. 2.

There are obvious difficulties and inaccuracies inherent in the application of experimental and theoretical data which deal largely with pure compounds when the Sangdong phases are clearly otherwise. However, the total salinity of much of the fluid is low and there is some experimental data on the effect on phase equilibria of changing phase composition (e.g. Burton et, al.
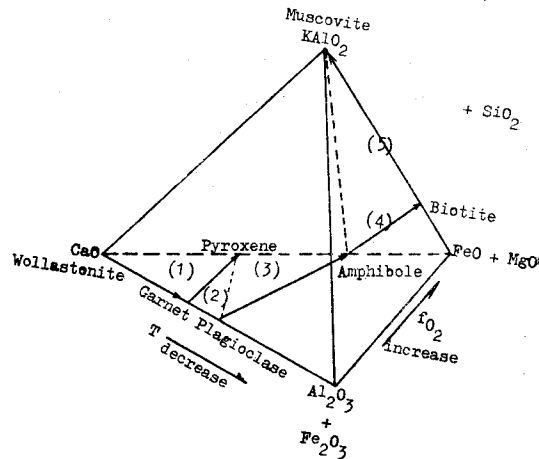

Fig. 2 Trends in the change of bulk chemistry and mineral assemblages at Sangdong skarns.
(1) Wollastonite-Andradite-Diopside
(2) Hedenbergite-Plagioclase-Garnet (grossularite-andradite)
(3) Hedenbergite-Plagioclase-Amphibole-Quartz   Amphibole-Quartz
(4) Amphibole-Biotite-Quartz Quartz-Biotite
(5) Muscovite-Biotite-Quartz Quartz-Muscovite-Chlorite

1982:Gamble, 1982). A more important question is whether any of the assemblages can be regarded as in equilibrium. The occurrence of near-monomineralic rocks and of consistent partition of elements between adjacent grains (e.g. Mg/Fe in hedenbergite and andradite) indicates a system at least near equilibrium. It is suggested that the gross mineralogical zones represent successive mineral assemblages formed in equilibrium with a fluid that is changing in composition as it migrates outwards from the feed zone. As the fluid at any point changes composition, overprinting results in coexistence of assemblages themselves more or less in equilibrium but in disequilibrium with hosts, and in this respect, considerable difficulties have been experienced in unravelling the paragenetic sequence at Sangdong, particularly in the pyroxene-garnet skarns. Overprinting by later fluids of different initial composition results in further complication (Moon, 1983).
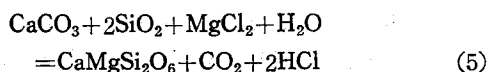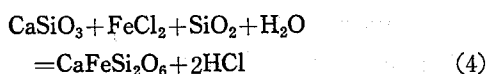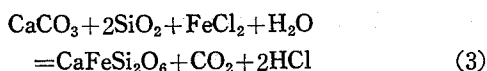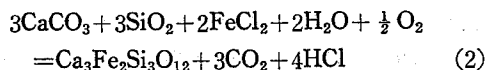
FORMATION OF EARLY SKARNS

There are mainly garnet-pyroxene-calcite rocks with or without wollastonite is explained by the well known reaction (Greenwood, 1967; Gustafson, 1974; Liou, 1974; Taylor & Liou, 1978):
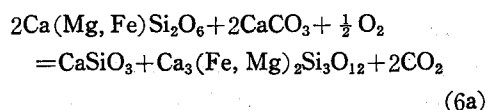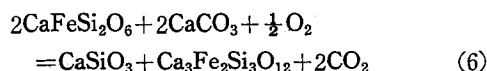
$$CaCO_3 + SiO_2 = CaSiO_3 + CO_2 \qquad (1)$$
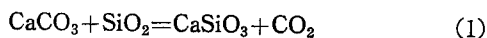
No fluid inclusions were found in this skarn, but the temperature of the formation of the wollastonite skarn can be estimated from P-T-X_{CO_2} data of Greenwood(1967), where X_{CO_2} is the mole fraction of CO_2. The limited fluid inclusion data indicate that the CO_2 mole fraction in the Sangdong skarns and in the veins was between 0.05 and 0.19. At $P_{total} = 1000$ bars and $X_{CO_2} = 0.1$, the equilibrium temperature is about 510°C, for $X_{CO_2} = 0.2$ the temperature is about 560°C(Shimazaki et al., 1973; Kerrick & Slaughter, 1976; Uchida & Iiyama, 1982). The T_h values (uncorrected) in the pyroxene-

garnet skarn near wollastonite-bearing skarn are 556°~580°C (specimens 106143 & 106149.).

To derive wollastonite skarn from limestone requires addition of silicon and other elements. These components were probably in part added to the circulatory fluid as a result of reaction between fluid and local shales. Wollastonite is most abundant in the Pungchon Limestone above the H1 skarn, where the primary fluids must have been considerably modified by circulation in the shales beneath the limestone. Where the activity of iron is high enough, andradite and hedenbergite are stable and where Mg becomes significant, diopside is stable. Potential reactions are:

$$3CaCO_3 + 3SiO_2 + 2FeCl_2 + 2H_2O + \tfrac{1}{2}O_2$$
$$= Ca_3Fe_2Si_3O_{12} + 3CO_2 + 4HCl \qquad (2)$$
$$CaCO_3 + 2SiO_2 + FeCl_2 + H_2O$$
$$= CaFeSi_2O_6 + CO_2 + 2HCl \qquad (3)$$
$$CaSiO_3 + FeCl_2 + SiO_2 + H_2O$$
$$= CaFeSi_2O_6 + 2HCl \qquad (4)$$
$$CaCO_3 + 2SiO_2 + MgCl_2 + H_2O$$
$$= CaMgSi_2O_6 + CO_2 + 2HCl \qquad (5)$$

The assemblage andradite-hedenbergite-calcite-wollastonite can be accommodated by the following reactions:

$$2CaFeSi_2O_6 + 2CaCO_3 + \tfrac{1}{2}O_2$$
$$= CaSiO_3 + Ca_3Fe_2Si_3O_{12} + 2CO_2 \qquad (6)$$
$$2Ca(Mg, Fe)Si_2O_6 + 2CaCO_3 + \tfrac{1}{2}O_2$$
$$= CaSiO_3 + Ca_3(Fe, Mg)_2Si_3O_{12} + 2CO_2$$
$$\qquad (6a)$$

For a given f_{CO_2}, the reaction is dependent on f_{O_2} and T. The early garnet(andradite)-pyroxene skarn contains calcite but little or no quartz and no wollastonite. This is compatible with the following reaction, with $a_{SiO_2} < 1$:

$$Ca_3Fe_2Si_3O_{12} + SiO_2 + CO_2$$
$$= 2CaFeSi_2O_6 + CaCO_3 + \tfrac{1}{2}O_2 \qquad (7)$$
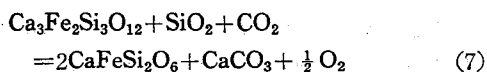
This reaction is thus dependent on both f_{O_2} and a_{SiO_2} for a given temperature and f_{CO_2}.

FORMATION OF LATER PYROXENE-GARNET SKARNS

In contrast to the wollastonite-bearing early pyroxene skarns, the minerals of the later skarns, Particularly hedenbergite, have abundant fluid inclusions. T_h values range from 580°C to 320°C, and average 418°C (Moon, 1983). It was concluded that T_h values>366°C required no correction but those below 366°C should be corrected for pressure, presumably of 800 bars. This yields a trapping temperature range of 390° to 600°C(?) for the late pyroxenes.

There is evidence in specimen 103118 (Moon 1983) of a temperature decline from early pyroxenes to later pyroxenes adjacent to amphibole-rich rock, T_h varying from>580°C to 395°C. T_h values also decrease away from the apparent fluid source near the margin of the skarn (Moon, 1983).

Reactions forming hedenbergite are important, as this is the dominant mineral. Apart from equation (4), in which wollastonite is replaced, hedenbergite may form by replacement of andradite:

$$Ca_3Fe_2Si_3O_{12}+SiO_2$$
$$\longrightarrow 2CaFeSi_2O_6+O_2+Ca^{2+} \qquad (8)$$
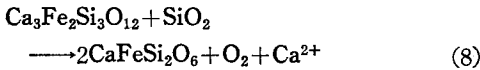
or, where with calcite, as per equation (7). Reaction (8) is dependent on $a_{Ca^{++}}$ for which there is no definitive information. The equilibrium assemblage hedenbergite-andradite-quartz-calcite is represented by equation (7) and plotted with respect to temperrature and f_{O_2} for X_{CO_2} values of 0.1 and 0.2 in Fig. 3. The low value of $X_{CO_2}(0.05)$ in the one skarn inclusion carrying CO_2 suggests 0.1 as the most likely value.

The tendency to develop monomineralic hedenbergite assemblages could result from decreases in f_{O_2} and $a_{Ca^{2+}}$ and/or an increase in a_{SiO_2}.

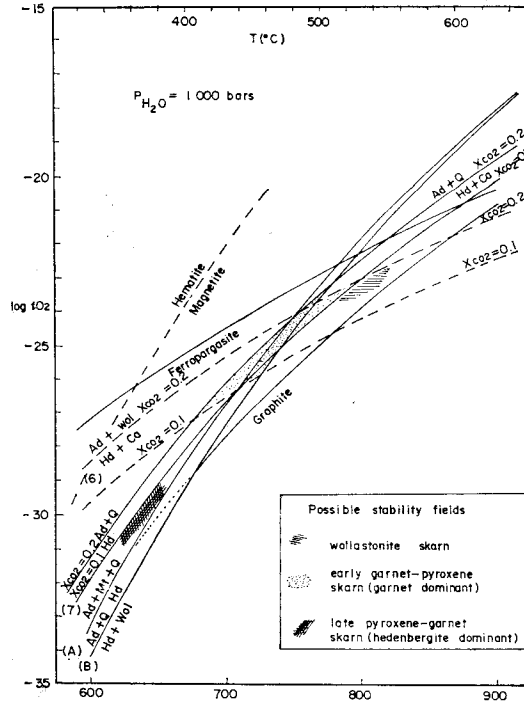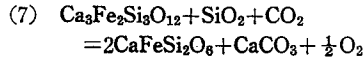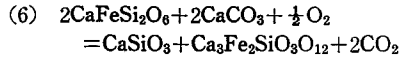In deeper levels of the M1 pyroxene-garnet zone, an assemblage of anorthite, grossular,

Fig. 3 Stability fields of the Sangdong skarns.
(6) $2CaFeSi_2O_6+2CaCO_3+\frac{1}{2}O_2$
$\qquad =CaSiO_3+Ca_3Fe_2Si_3O_{12}+2CO_2$
(7) $Ca_3Fe_2Si_3O_{12}+SiO_2+CO_2$
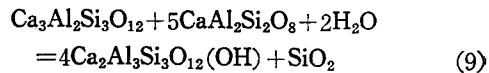$\qquad =2CaFeSi_2O_6+CaCO_3+\frac{1}{2}O_2$
Curve (A) from Burton et al.(1979)
Curve (B) from Gustafson(1974)
Curve for ferropargasite from Gilbert(1966)
Curve for graphite from French(1966)

quartz, clinozoisite and hedenbergite is present, with hedenbergite undergoing replacement. A possible equilibrium is:

$$Ca_3Al_2Si_3O_{12}+5CaAl_2Si_2O_8+2H_2O$$
$$=4Ca_2Al_3Si_3O_{12}(OH)+SiO_2 \qquad (9)$$

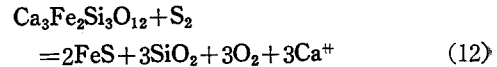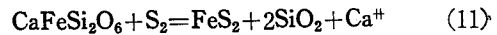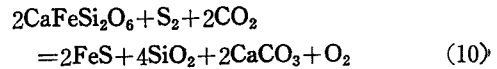The plagioclase is about 0.9 mole% anothite. Using Bird and Helgeson's(1981) phase relations for the $CaO-FeO-Fe_2O_3-Al_2O_3-SiO_2-HCl-H_2O$ system at 400°C, 1kb and $a_{H_2O}=1$, and the composition of two epidote samples of $X_{Ca_2Fe_3Si_3O_{12}(OH)}=0.13$ and 0.26 (Moon, 1983), the calcium content of the fluid can be loosely constrained as follws:

$$\log a_{Ca^{2+}}/(a_{H^+})^2=5.7 \text{ to } 6.6$$

The sulphides in the pyroxene-garnet skarns appear to be later than the early silicates and later than much of the later silicates. Some sulphides have formed at the same time as pyroxene as seen in specimen 103166 (Moon, 1983), where pyrite, hedenbergite and quartz appear to have grown together. It thus seems likely that quartz, scheelite, sulphides and some pyroxenes formed together fairly late in the evolution of the skarn. The low T_h values of some quartz in the skarn indicate quartz deposition continued to very late stages.

Pyrrhotite is the most abundant sulphide and replaces pyroxnes but pyrite is locally present (without pyrrhotite) and in a few specimens magnetite is present (no sulphides in contact). Possible sulphidation reactions are:

$$2CaFeSi_2O_6 + S_2 + 2CO_2$$
$$= 2FeS + 4SiO_2 + 2CaCO_3 + O_2 \quad (10)$$
$$CaFeSi_2O_6 + S_2 = FeS_2 + 2SiO_2 + Ca^{++} \quad (11)$$
$$Ca_3Fe_2Si_3O_{12} + S_2$$
$$= 2FeS + 3SiO_2 + 3O_2 + 3Ca^{++} \quad (12)$$

The experiments of Gamble(1982) and Burton et al.(1982) provide useful data on the influence of varying silicate composition. Taking Sangdong hedenbergite as having a mole fraction of diopside of 0.26 and of johannsenite of 0.06 (Moon, 1983) indicates that pyrite could only form below 376°C at 1kb pressure(Fig. 4). If the application of the pressure correction to the lower T_h values in pyroxenes is correct then pyrite must be later (at lower temperature)
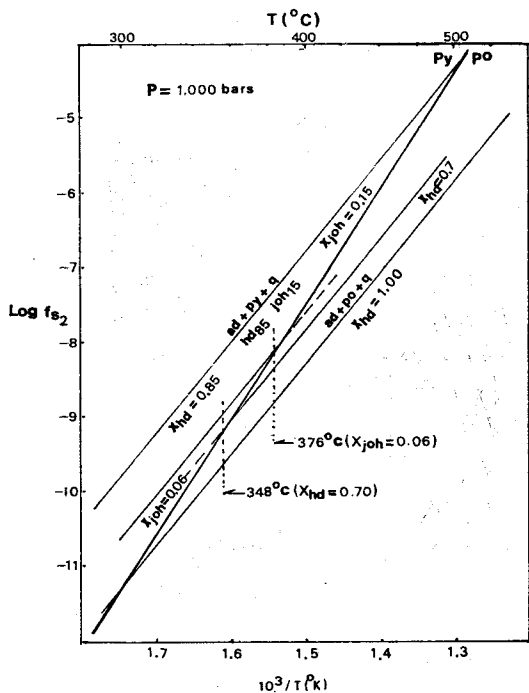
Fig. 4 Stability fields for pyrite, pyrrhotite, hedenbergite and andradite.
Stability of hedenbergite(hd) and andradite (ad) is based on Burton et al.(1982) and Gamble(1982).
Average $X_{hd} = 0.7$, $X_{dip} = 0.26$ and $X_{joh} = 0.06$ are based on
dip=diopside   joh=johannsenite
py=pyrite   po=pyrrhotite   Q=quartz
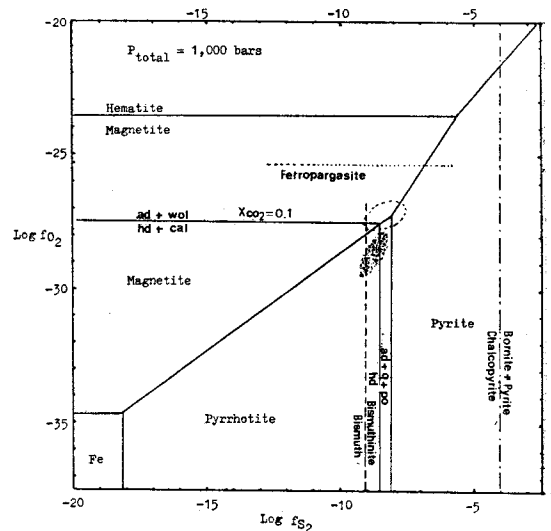
Fig. 5 Estimate of conditions during late pyroxene-garnet skarn and amphibole skarn formation in terms of f_{O_2}–f_{S_2} at 400°C.
The stippled area indicates the environment of late pyroxene-garnet skarn mineralization. The stability field of hedenbergite is from eq. (6) and Burton et al(1979). The equilibria are calculated from data of Robie et al. (1978)
⊂⊃-stability fields of amphibole and mica skarns formation. The stability field of ferropargasite is from Gilbert(1966).

than most of the silicates. Combining this with the bulk of the petrographic evidence indicates that the sulphides probably formed at a very late stage in pyroxene-garnet skarn evolution and to some extent, later than the silicates. The abundance of pyrrhotite and relatively scarce non-coexisting, pyrite and magnetite, indicate $f_{O_2}-f_{S_2}$ conditions mainly in the pyrrhotite field at 400°C but not far removed from pyrite and magnetite stability (Fig. 5). Coexisting bismuth and bismuthinite provide a useful constraint on f_{S_2}.
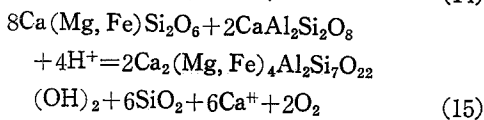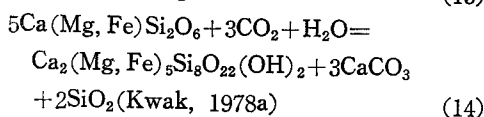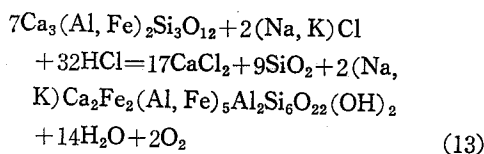
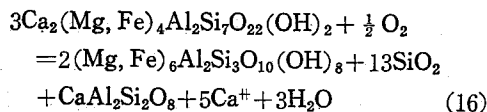## FORMATION OF THE BIOTITE AND AMPHIBOLE SKARNS

These skarns appear to exist in chemical and textural equilibrium. At the "front" of the amphibole zone, however, there is clear evidence of replacement, and amphibole occurs in veins, veinlets and patches anastomosing the pyroxene-garnet rock. Three possible reactions producing tremolite, hastingsitic hornblende, ferroedenitic hornblende and ferro-hornblende are shown here:

$$7Ca_3(Al, Fe)_2Si_3O_{12}+2(Na, K)Cl$$
$$+32HCl=17CaCl_2+9SiO_2+2(Na,$$
$$K)Ca_2Fe_2(Al, Fe)_5Al_2Si_6O_{22}(OH)_2$$
$$+14H_2O+2O_2 \qquad (13)$$
$$5Ca(Mg, Fe)Si_2O_6+3CO_2+H_2O=$$
$$Ca_2(Mg, Fe)_5Si_8O_{22}(OH)_2+3CaCO_3$$
$$+2SiO_2(Kwak, 1978a) \qquad (14)$$
$$8Ca(Mg, Fe)Si_2O_6+2CaAl_2Si_2O_8$$
$$+4H^+=2Ca_2(Mg, Fe)_4Al_2Si_7O_{22}$$
$$(OH)_2+6SiO_2+6Ca^++2O_2 \qquad (15)$$

These reactions release calcium to the fluid, causing precipitation of calcite and scheelite. The production of oxygen may explain the abundance of magnetite(with pyrrhotite and pyrite), particularly at the amphibole "front".

Chlorite is abundant in much of this skarn replacing amphibole. Both the chlorite and amphibole appear to accompany fluorite, quartz, and scheelite. The replacement of amphibole by chlorite can be represented by the following reaction:

$$3Ca_2(Mg, Fe)_4Al_2Si_7O_{22}(OH)_2+\tfrac{1}{2}O_2$$
$$=2(Mg, Fe)_6Al_2Si_3O_{10}(OH)_8+13SiO_2$$
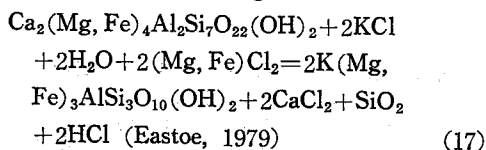$$+CaAl_2Si_2O_8+5Ca^++3H_2O \qquad (16)$$

Again, calcium is released to the fluid, allowing precipitation of calcite, scheelite and fluorite.

Only two specimens of amphibole have yielded fluid inclusions and these have T_h values ranging from 287 to 307°C and indicate somewhat lower temperatures than in the pyroxene-garnet skarn. Uncorrected T_h values in coexisting scheelite have a similar range to these in the pyroxene garnet skarn zone suggesting a fairly constant temperature across the boundary in later stages. There is no evidence of boiling within the amphibole association, so a range of trapping temperatures for the assemblage is from a maximum of 500°C for scheelite down to about 250°C for quartz(Moon, 1983).

Pyrrhotite and magnetite, native bismuth and bismuthinite occur as coexisting pairs in the amphibole skarn, associated with amphibole and/or chlorite. These assemblages provide a fairly tight constraint on the range of f_{O_2} and f_{S_2} in these rocks(Fig. 5), and suggest the sulphides(with scheelite, chlorite?) formed in slightly higher oxidation conditions compared to these of the late pyroxene-garnet skarn.

The f_{O_2} value is consistent with the upper stability limit of ferropargasite determined by Gilbert(1966), as shown in Fig. 3 and 5.

The biotite-amphibole equilibrium can be expresssed by the following reaction:

$$Ca_2(Mg, Fe)_4Al_2Si_7O_{22}(OH)_2+2KCl$$
$$+2H_2O+2(Mg, Fe)Cl_2=2K(Mg,$$
$$Fe)_3AlSi_3O_{10}(OH)_2+2CaCl_2+SiO_2$$
$$+2HCl \text{ (Eastoe, 1979)} \qquad (17)$$

Two inclusions in biotite have T_h values of 381°C and 286°C which pressure correct to 480°C and 365°C approximately. Scheelite trapping temperatures for this skarn range from

600°C to 300°C and quartz from 460°C to 220°C. The high T_h value of scheelite inclusions (specimen 106044) coincides with a T_h in adjacent pyroxene of 580°C.

Purtscheller and Rammlmair (1982) have empirically and qualitatively correlated the partitiion of Mg and Fe between amphibole and biotite in a metamorphic terrain. Comparable data from specimen 103109. indicates a minimum equilibration temperature a little below 400°C.

Bismuthinite and bismuth, pyrrhotite and magnetite occurring with biotite again loosely constrain f_{O_2} and f_{S_2} conditions (Fig. 5). The volume % native bismuth/bismuthinite ratio increases outward from the mica skarn, roughly confirming with a trend to lower f_{O_2} and f_{S_2} in that direction.

Although the arrangement biotite-amphibole-pyroxene+garnet is the usual one at all scales, biotite in contact with pyroxene-garnet has been observed as a quartz-mica skarn veining the pyroxene-garnet skarn and surrounding dyke
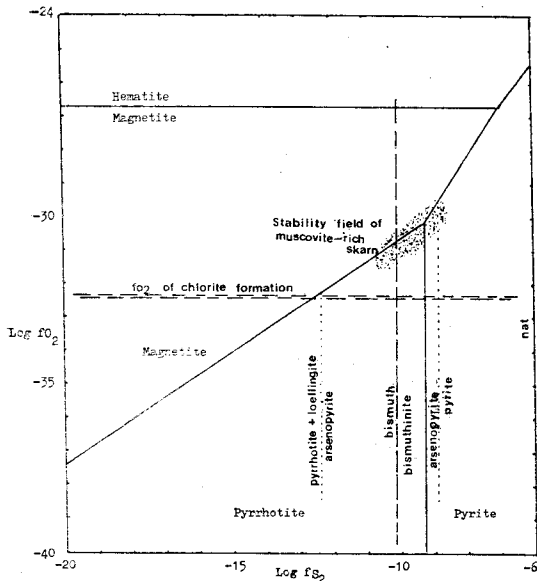
Fig. 6 Estimate of conditions of muscovite-rich skarn formation in the system Fe-O-S on an $f_{S_2}-f_{O_2}$ diagram at 350°C.
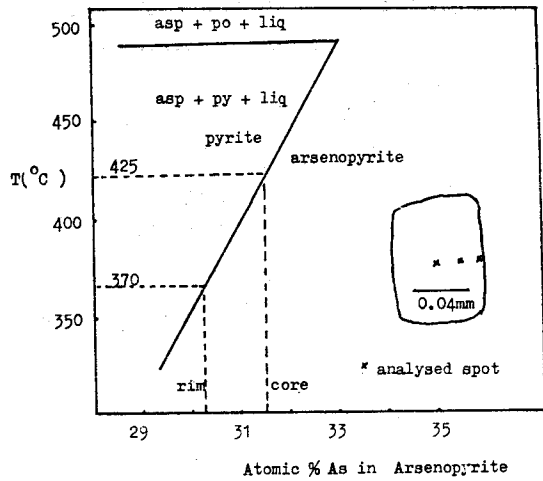
Fig. 7 Estimate of formation temperature from atomic % As in arsenopyrite (from Kretschmar and Scott, 1976).
asp=arsenopyrite   liq=liquid
py=pyrite   po=pyrrhotite

in the pyroxene-garnet skarn (at -12th level). The reactions involved can be expressed as:

$$3Ca(Mg, Fe)Si_2O_6 + Ca_3(Al, Fe)_2Si_3O_{12}$$
$$+ K^+ + 2H = K(Mg, Fe)_3AlSi_3O_{10}(OH)_2$$
$$+ 6SiO_2 + 6Ca^{++} + 3O_2 + Fe^{3+} \qquad (18)$$
$$6Ca(Mg, Fe)Si_2O_6 + CaAl_2Si_2O_8 + 2K^+$$
$$+ 12H^+ = 2K(Mg, Fe)_3AlSi_3O_{10}(OH)_2$$
$$+ 8SiO_2 + 7Ca^{++} + 4H_2O \qquad (19)$$
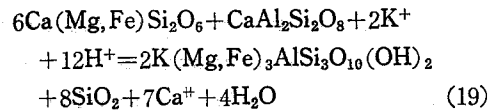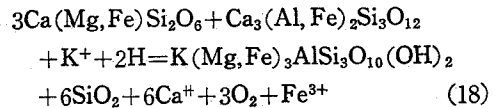
FORMATION OF THE QUARTZ-MUSCOVITE-CHLORITE SKARN

This skarn appears to have been derived from the biotite skarn by alteration. It is unusual in containing small amounts of wolframite, hematite and arsenopyrite. The arsenopyrite occurs with pyrite. The composition of the arsenopyrite indicates a temperature range of 370°C to 425°C from rim to core (Fig. 7) and log f_{S_2} of -6 to -7.4 (using data of Kretschmar and Scott, 1976).

The presence of hematite in one specimen (106174) with magnetite and pyrite indicates an oxidation state too high to be compatible with the presence of bismutinite, pyrrhotite and

arsenopyrite, and it may be a very late phase. Possible chemical reactions to form this skarn are as follows:

$$5K(Mg,Fe)_3AlSi_3O_{10}(OH)_2+22HCl$$
$$=KAl_3Si_3O_{10}(OH)_2+(Mg,Fe)_6Al_2$$
$$Si_3O_{10}(OH)_8+4KCl+6FeCl_2$$
$$+3MgCl_2+9SiO_2+11H_2O+\tfrac{1}{2}O_2 \quad (20)$$
$$3CaAl_2Si_2O_8+4H^++2K^+$$
$$=2KAl_2AlSi_3O_{10}(OH)_2+3Ca^{++} \quad (21)$$
$$3Ca_3Al_2Si_3O_{12}+4H^++2K^+$$
$$=2KAl_3Si_3O_{10}(OH)_2+3SiO_2$$
$$+9Ca^{++}+3O_2 \quad (22)$$
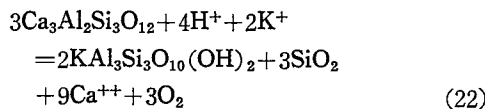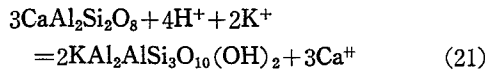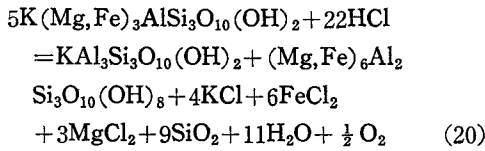
Equation (21) represents replacement of plagioclase in the footwall-side cherty rock by muscovite skarn in the quartz-mica zone, and equation (22) represents the formation of the quartz-muscovite skarn in parts of the F. orebody. All result in decrease of acidity in the fluid.

Development of muscovite is associated with precipitation of scheelite and quartz. Corrected temperatures of homogenization of scheelite inclusions range from values compatible with the arsenopyrite temperature down to about 300°C while quartz precipitation apparently continues to even lower temperatures.

The highest T_h values in scheelite occur in the mica skarn in the lower mine levels and T_h values of quartz show a pronounced high in the core of the mica skarn and a low coinciding with the late muscovite-chlorite skarn. The muscovite skarn thus appears to be a lower temperature, late stage assemblage. Later activity appears to involve hematite and quartz; in addition, calcite is seen replacing muscovite and T_h values of fluorite inclusions indicate low temperature, hence late precipitation.

The wolframite in specimen (106174) has a very low manganese content, and unlike wolframite in quartz veins occurs with calcite and magnetite. Possible reactions are as follows:

$$3CaWO_4+Fe_3O_4+3CO_2$$
$$=3FeWO_4+3CaCO_3+\tfrac{1}{2}O_2 \quad (23)$$
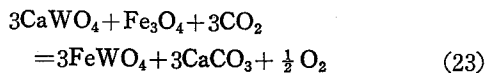
Rose and Burt(1979) explained the presence of scheelite and ferberite by a reaction involving fluorine:

$$Fe_3O_4+3CaWO_4+3F_2O_{-1}$$
$$=3CaF_2+3FeWO_4+\tfrac{1}{2}O_2 \quad (24)$$
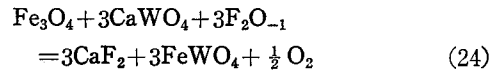
The common occurrence of fluorite and scheelite in the Sangdong skarns, the close association in the veins of wolframite and scheelite commonly without fluorite, and the replacement of muscovite by calcite indicate the first reaction seems to be more pertinent at Sangdong and that f_{CO_2} is critical. The T—f_{O_2}—X_{CO_2} dependence of these reactions are plotted in Fig. 8, using scheelite data from Robie et al(1978). The f_{O_2} values for the likely mole % CO_2 in solution are too clearly too high, indicating problems with the thermodynamic data.
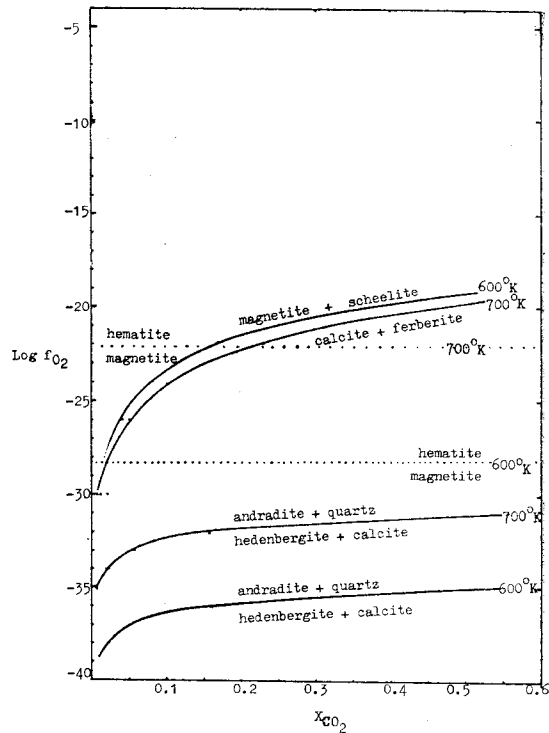
The presence of muscovite allows a crude

Fig. 8 Comparison of conditions of formation between proxene-garnet skarn and quartz-muscovite skarn in which ferberite, magnetite, calcite and scheelite occur.

estimate of pH in the fluids. Leachate analyses of fluid inclusions in tin-tungsten deposits apparently derived from granitoid magmas indicate m_{K^+} of about 0. 1 at temperatures of 300~400°C, e.g.
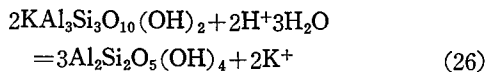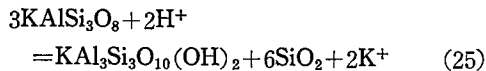
Cligga Head(Charoy, 1979)

m_{K^+}	T(°C)
0. 1—0. 17	300—450

Renison(Patterson et al., 1981)

0. 2	350

Using, say, $m_{K^+}= 0. 1$ at 350°C indicates that the pH was between 4. 2 and 5. 9 because there is little or no kaolinite or K-felspar in this skarn. The appropriate reactions are:

$$3KAlSi_3O_8+2H^+$$
$$=KAl_3Si_3O_{10}(OH)_2+6SiO_2+2K^+ \quad (25)$$
$$2KAl_3Si_3O_{10}(OH)_2+2H^+3H_2O$$
$$=3Al_2Si_2O_5(OH)_4+2K^+ \quad (26)$$

At 350°C, neutral pH is 5. 7 so the solutions are neutral to acid.

The mineralogy and other constraints can be used to indicate a likely value for the molality of total sulphur. In Fig. 9 the oxidation state is shown as $\sum SO_4/\sum H_2S$ where

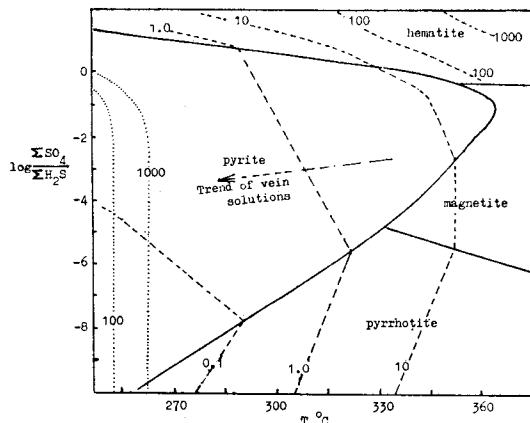$$\sum SO_4=SO^{2-}_4+HSO^-_4+NaSO^-_4$$
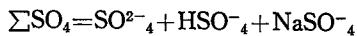
Fig. 9 Log($\sum SO_4/\sum H_2S$) versus T diagram displaying the possible fields of formation of sulphide minerals in the hydrous (amphibole-rich and mica rich) skarns. $m_{\sum S}=2.5\times10^{-3}$.
Key: ----, ppm Cu (solubilty of Cu)
······, ppm Zn (solubilty of Zn)
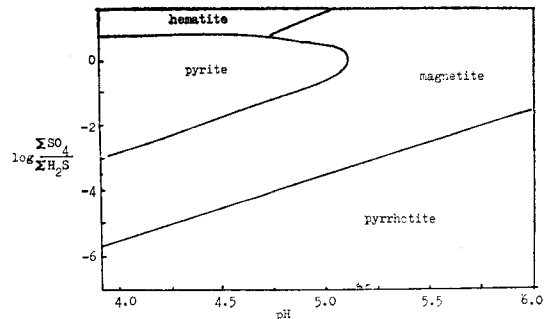
Fig. 10 Log($\sum SO_4/\sum H_2S$) versus pH (at 350°C) diagram. $m_{\sum S}=2.5\times10^{-3}$.

$$+KSO^-_4+MgSO^-_4+CaSO^-_4$$
$$\sum H_2S=H_2S+HS^-+S^{2-}$$
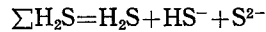
The diagram is calculated using a programme prepared by Ripley & Ohmoto(1980) and modified by J.L. Patterson and G.R. Green at the University of Tasmania.

The fluid is assumed to have the following characteristics:

pH=4, m_{K^+}=0. 1. m_{Na^+}=0. 85, $m_{Mg^{++}}$
=0. 014, m_{Cl^-}=1. 00, m_{Ca}=0. 00
m_{Cu}=$10^{-9.00}$, m_{Mn}=10^{-7}, $m_{\sum C}$=0. 10.

Manipulating values of $m_{\sum S}$ gives a reasonable fit at $m_{\sum S}=2.5\times10^{-3}$. in Fig. 10, the temperature is fixed at 350°C and conditions other than pH are as for 9.

FORMATION OF CHLORITE

Walshe and Solomon(1981) have developed a model involving substitutions in chlorite to obtain estimates of the temperature and f_{O_2} at which the chlorite assemblages equilibrate.

Among the common six end-members of the chlorites, only four could be used to represent Sangdong chlorites, viz.

$$Mg_5AlSi_3AlO_{10}(OH)_8+5/3Fe_3O_4+10/3SiO_2$$
$$+10/3H_2O=Fe^{++}_5AlSi_3AlO_{10}(OH)_8$$
$$+5/6Mg_6Si_4O_{10}(OH)_8+5/6O_2$$
$$(27)$$
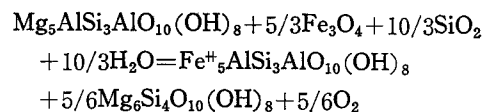
for which $\cdot$log K=$\log a_3$+5/6$\log a_1$+5/6log(f_{O_2}) $-\log a_2$ where a_1(=activity) of the thermodynamic

Table 1 Chlorite structural formulae.

	Specimen 103120	Specimen 103119
Mg^{+2}	0.801	1.027
Mn^{+2}	0.039	0.063
Fe^{+2}	3.841	3.614
Fe^{+3}	0.104	0.108
Al^{+3}	1.215	1.188
Si^{+4}	2.681	2.704
Al^{+3}	1.319	1.296
Total	10.000	10.000
O	10.000	10.000
OH	8.000	8.000
$Mg/(Mg+Fe)$	0.169	0.216
Fe^{+3}/Fe^{+2}	0.014	0.014

Mole Fraction		
$Mg_6Si_4O_{10}(OH)_8$	-0.326	-0.572
$Mg_4Al_2Si_3O_{10}(OH)_8$	0.551	0.913
$Fe_5{}^{2+}Al_2Si_3O_{10}(OH)_8$	0.716	0.484
$Fe_5{}^{2+}Fe_2{}^{3+}Si_3O_{10}(OH)_8$	0.052	0.109

component $Mg_6Si_4O_{10}(OH)_8$, a_2(=activity) of the thermodynamic component $Mg_5AlSi_3AlO_{10}(OH)_8$, and a_3(=activity) of the thermodynamic component $Fe_5{}^{2+}AlSi_3AlO_{10}(OH)_8$ Chlorites analyzed by microprobe are given in Table 1 for two samples(103120 and 103119) from the quartz-mica skarn. The chlorite and magnetite occur in a specimen from the quartz-muscovite-chlorite rock but they are not quite in contact.

The f_{O_2} values obtained from the above equation are as follows;

Temperature (°C)	specimen 103120	specimen 103119
250	-38.72	-38.84
300	-35.31	-35.42
350	-32.37	-32.48

These results indicate the formation of chlorite may take place at f_{O_2} condition slightly lower than the mica assemblage at 350°C.

CONCLUSION (THE EVOLUTION OF SKARNS)

Recent drillings into the Janggsan Quartzite

and the Precambrian schist about 500m below the 3rd level an intrusive pluton has been encountered at Sangdong (Yoon, 1984). The age of the deposit (Farrar et al., 1978) appears to be about 81~84 Ma, a period in which magmatism took place nearby and magmatic tungsten mineralization formed in other parts of Korea (e.g 80 to 96 Ma at the Sannae Mine, Ihihara et al., 1981). Magmatic tungsten mineralization also developed at about this time in Japan (64 to 96 Ma, Shibata and Ishihara, 1974), at the Yukon (80 to 92 Ma, Dick and Hodgson, 1982), at pine Creek (74 to 87 Ma, Gray et al., 1968), and at Vostok in Russia (84 Ma, Levarshev, 1972). Most tungsten deposits
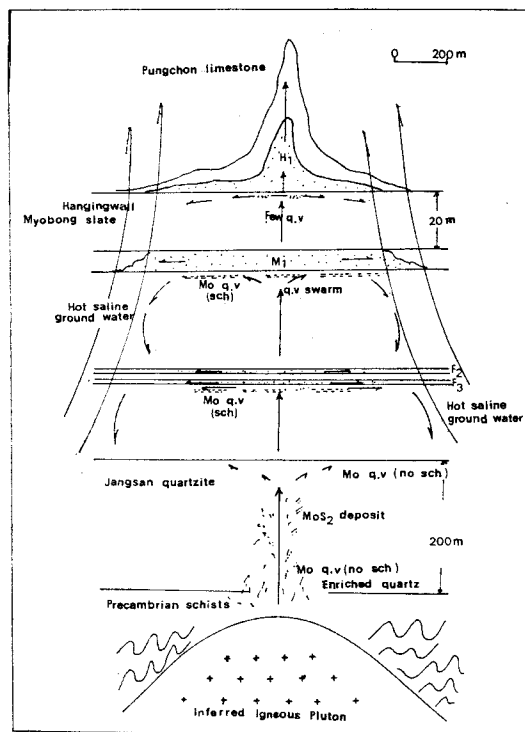

Fig. 11 Diagrammatic vertical section of Sangdong skarns showing fluid circulation.
Few q.v=very few quartz veins are developed in hangingwall slate, q.v=quartz vein, Mo=molybdenite, Enriched quartz= strong silicification at the bottom of the Jangsan quartzite may be responsible for increasing the thickness of the quartzite, (sch)=quartz veins contains scheelite.
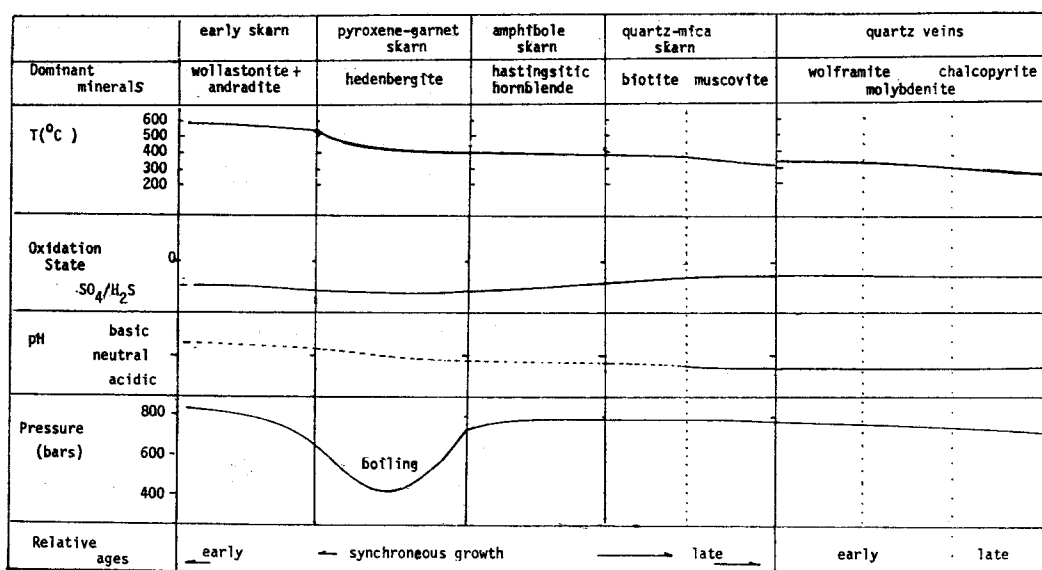
	early skarn	pyroxene–garnet skarn	amphibole skarn	quartz-mica skarn	quartz veins	
Dominant minerals	wollastonite + andradite	hedenbergite	hastingsitic hornblende	biotite muscovite	wolframite chalcopyrite molybdenite	
T(°C) 600 500 400 300 200						
Oxidation State SO_4/H_2S						
pH basic neutral acidic						
Pressure (bars) 800 600 400		boiling				
Relative ages	early	← synchroneous growth		→ late	early	late

Fig. 12 Generalized conditions of evolution of the Sangdong deposit.

(e.g. Pine Creek, MacTung, Ming Island, Salau) are clearly related to granitoid plutons and a similar situation is inferred from mineralogy and fluid inclusions, and the oxygen-and sulphur-isotope ratios inferred for the fluids, all point to the presence of a substantial pluton beneath the mine. There is no evidence of an enrichment of tungsten in the rocks, as suggested by Kim (1976), and the mineralization is regarded as epigenetic. The closure of the outer skarns when drawn in the plane of the M_1 orebody and distribution of the quartz veins indicates the location of a rising plume of hot fluid (Fig. 11).

The fluid appears to have moved up a NE fracture zone (Moon, 1983) that controls the orientation of the skarn zones and the distribution of T_h values in the mica-amphibole zones. Analysis of groundwater circulation during cooling of plutons by Norton and Knight (1977) indicates that it is difficult to raise ground temperatures sufficiently high to form wollastonite-bearing skarns at a distance of 0.5km from a pluton boundary in a uniformly permeable medium. To achieve the required temperature distribution and maintain temperatures 400°C during growth of the hydrous skarn appears to require fluid transfer in faults or zones of highly permeable strata.

It is also clear that the rocks beneath the ore horizon must have been chemically inert in the sense that solution acidity was not affected, and a fairly reduced condition was maintained.

The skarn zones are believed to evolve as follows (see Figs. 11 & 12).

1) During or immediately preceding emplacement of the inferred pluton, the rocks of the mine area are warmed by groundwater circulating as a result of magmatic heating. This short-lived phase seems inevitable though there is no specific evidence for it. At King Island, Kwak (1978b) found relatively low temperature, low salinity fluids in the cores of garnet crystals that preceded the development of saline, high temperature fluids.

2) With increased temperature a zone of wollastonite-bearing garnet-pyroxene skarn developed, about 1.5km×1.2km×0.5km in extent. The temperature probably ranged from 510°C to 560°C and reaction involvig fluid, limestone and

slate occurred with increasing chemical mobility of elements such as Mg, Fe, Ca and CO_2.

3) Development of the early pyroxene-garnet skarn merged to a phase involving solutions of essentially magmatic origin.

Reaction with the early skarn resulted in the development of the mica, amphibole, and late pyroxene-garnet skarns by diffusion+infiltration metasomatism. The resulting mineralogical zones grew outward from the central area of the hot plume, widening with time, leaving relics of earler skarn throughout the deposit. Small scale zonation along fractures shows a similar evolutionary patten.

The later pyroxene-garnet skarns have fluid inclusions showing evidence of boiling and T_h values range from 313°C to 580°C (average 418°C). Likely pressures for a NaCl-H_2O system are 400 bars at 400~500°C but there is insufficient data for the more complex natural system (NaCl-KCl-$CaCl_2$ $MgCl_2$-H_2O) to determine quantitative pressures. A hydrostatic regime is inferred for this stage, possibly brought about by tectonic fracturing of the overburden. No evidence of boiling is seen in the lower temperature members of this assemblage, indicating a sealing of the system and a reversion to lithostatie pressure, tentatively estimated at 800 bars from sphalerite compositions. Lack of gas-dominated inclusions in the mica-and amphibole-rich skarns and the veins indicates similar lithostatic conditions in these rocks. It is concluded that the skarns formed from boilhg solutions are slightly earlier (and higher temperature) than the others. The inferred hydrostatic conditions may have given way to lithostatic possibly by sealing of fractures due to mineral precipitation.

The data are inadequate to identify temperature gradients within the skarn but a decline is seen close to the country rock contacts. To maintain a sharp boundary with steep temperature and chemical gradients probably requires

double-diffusive mechanisms, such as advocated by Eastoe (1979) for porphyry copper systems. In this model the mass of hot, magmatic fluid is contained within an envelope of hot groundwater of contrasting salinity during the life of individual surges of ore fluid. Similar (see Fig. 11) conditions could prevail in the Sangdong aureole with a hot, low salinity groundwater that gradually or occasionally mixes and becomes incorporated into the ore system. The incoming ore fluid during this period has the following general characteristics:

T   313°~600°C(?)
$m_{\Sigma S} \approx 2.5 \times 10^{-3}$
pH $\approx$ 4.0 at350°C $f_{O_2} \approx 10^{-23} \sim 10^{-31}$
X_{CO_2} 0.1mole(?) $f_{S_2} \approx 10^{-9} \sim 10^{-12}$
$\delta^{34}S_{H_2S}$ 4.5~5.3 permil
$m_{Ca^{++}} < 10^{-6}$mole(inferred)
$\delta^{18}O_{H_2O}$ 6.6~8.5 permil
$m_{K^+} \approx 10^{-1}$mole(by analogy)
$\delta^{13}O_{CO_2}$-5.3~0.9 phrmil

There is a clear trend of declining temperature with time, from $T > 500$°C for the early skarns to 300°C or so for the final muscovite skarn in the core of the deposit.

The $a_{Ca^{++}}$ may increase during the life of an individual packet of fluid moving through the skarn zones by reactions with amphibole and pyroxene skarns, and possibly by localized recirculation of fluids that have reacted with carbonates. These factors may account for a change from wolframite-rich veins to sceelite-bearing skarns.

The major overall changes involved in developing the skarns are addition of FeO, MnO, K_2O, SiO_2, Al_2O_3, WO_3 and H_2O to the rocks and loss of CaO.

Equilibrium with the incoming ore fluid was approached in the development mucovite-rich assemblage in the core of the deposit, at temperatures of about 350°C or 400°C. Chloritization of biotite are amphibole probably took place in

these later stages of skarn growth.

Quartz-molybdenite and quartz-wolframite veins formed in footwall rocks and around the skarn during skarn growth. T_h values of vein and skarn are similar, and overall P-T-X conditions for the vein appear to the skarns. The relationships between molybdenite and wolframite veins are not clear.

4) Quartz precipitation continued to relatively low temperatures (290° to 350°C) throughout the skarn and in the late veins. These veins cut the skarn, are sulphide-rich, particularly in chalcopyrite, and carry sphalerite and galena. The solutions generally are of similar composition to earlier solutions and appear to be still largely ot magmatic origin. Some recycling of scheelite and precipitation of low Mo-scheelite occurred at this time.

5) Later stages of fluid circulation involved formation of quartz and calcite, and locally hematite, at temperature $\leqslant$250°C. $\delta^{13}C$ data of calcite from a molybdenite-bearing calcite vein indicate the involvement of nonmagmatic fluid.

REFERENCES

Barlin, I., Knacke, O. and Kubaschewski, O. (1977) Thermochemical properties of inorganic substances. v. 1 & 2. Springer-Verlag.

Bird, D.K. and Helgeson, H.C. (1981) Chemical interaction of aqueous solutions with epidote-feldspar mineral assemblages in geologic systems. II: equilibrium constraints in metamorphic/geothermal.

Burton, J.C., Taylor, L.A. and Chou, I.M. (1982) Determination of the f_{O_2}-T stability relations of hedenbergite and hedenbergite-johannsenite solid solutions by the hydrogen fugacity sensor technique. Econ. Geol., v. 77, p. 764-783.

Charoy, B. (1979) Greisenisation et fluides associes a Cligga Head, Cornwall (sud-ouest de l'Agleterre). Bull. Mineral, v. 102, p. 633-641.

Dick, L.A. and Hodgson, C.J. (1982) The MacTung W-Cu(Zn) contact metasomatic and related deposits of the Northeastern Canadian Cordillera. Econ.

Geol., v. 77, p. 845-867.

Eastoe, C.J. (1979) The formation of the Panguna porphyry copper deposit, Bougainville, Papua New Guinea. Unpub. Ph.D. thesis, University of Tasmania, Australia. 255p.

Farrar, E., Clark, A.H. and Kim, O.J. (1978) Age of the Sangdong tungsten deposit, Republic of Korea, and its bearing on metallogeny of the southern Korean peninsula. Econ. Geol., v. 73, p. 547-566.

Gamble, R.P. (1982) An experimental study of sulfidation reactions involving andradite and hedenbergite. Econ. Geol., v. 77, p. 784-797.

Gilbert, M.C. (1966) Synthesis and stability relations of the hornblende, ferropargasite. Am. J. Sci., v. 264, p. 698-742.

Gray, R.F., Hoffman, V.J., Bagan, R.J. and McKinley, H.L. (1968) Bishop tungsten district, California. In: Ridge, J.D. (ed.) Ore Deposits of United States 1933~1967. v. 2, p. 1532-1554.

Greenwood, H.J. (1967) Wollastonite: stability in H_2O-CO_2 mixtures and occurrence in a contact-metamorphic aureole near Salmo, British Columbia, Canada. Am. Mineral., v. 52, p. 1669-1680.

Gustafson, W. (1974) The stability of andradite, hedenbergite and related minerals in the system Ca-Fe-Si-O-H. J. Petrol., v. 15, p. 455-496.

Guy, B. (1979) Petrologie et geochemie isotopique (S, C, O) des skarns a scheelite de Costabonne, Pyrenees-Orientales, France (English abstract, 11p). Unpub. Ph.D. thesis, 238p.

Helgeson, H.C. (1969) Thermodynamics of hydrothermal systems at elevated temperatures and pressures. Am. J. Sci., v. 267, p. 729-804.

Helgeson, H.C., Delany, J.M., Nesbitt, H.W. and Bird, D.K. (1978) Summary and critique of the thermodynamic properties of rock-forming minerals. Am. J. Sci., v. 278(A), p. 1-229.

Kim, S.Y. (1976) Geology, mineralogy and geochemistry of tungsten deposits of the Sangdong-Ogbang area, South Korea. Unpub. Ph. D. thesis, University of Leed, U.K., 346p.

Korzhinskii, D.S. (1968) The theory of metasomatic zoning. Mineral Deposita, v. 3, p. 222-231.

Korzhinskii, D.S. (1970) Theory of metasomatic

zoning. London. Oxford University Press.

Kretschmar, U. and Scott S.D. (1976) Phase relations involving arsenopyrite in the system Fe-As-S and their application. Can. Miner., v. 14, p. 364-386.

Kwak, T.A.P. (1978a) Mass balance relationships and skarn forming processes at the King Island scheelite deposit, King Island. Tasmania, Australia. Am. J. Sci., v. 278, p. 943-968.

Kwak, T.A.P. (1978b) The conditions of formation of the King Island scheelite contact skarn, King Island, Tasmania, Australia. Am. J. Sci., v. 278, p. 969-999.

Levashev. G.B., Govorov, I.N., Strizhkova, A.A. and Grechischeva, A.P. (1972) The regional geochemistry of tungsten in Primorye. Geochem. Inst., v. 9, p. 279-293.

Liou, J.G. (1974) Stability relations of andradite-quartz in the system Ca-Fe-Si-O-H. Am. Miner., v. 59, p. 1016-1025.

Moon, K.J. (1983) The Genesis of the Sangdong Tungsten Deposit, the Republic of Korea. Unpub. Ph. D. thesis, University of Tasmania, Australia.

Newberry, R.J. (1982) Tungsten-bearns of the Sierra Nevada. 1. The Pine Creek Mine, California. Econ. Geol., v. 77, p. 823-844.

Norton, D. and Knight, J. (1977) Transport phenomena in hydrothermal systems, cooling plutons. Am. J. Sci, v. 277, p. 937-981.

Patterson, D.J. (1979) Geology and mineralization at Renison Bell, western Tasmania. Unpub. Ph. D. thesis, University of Tasmania.

Purtscheller, F. and Rammlmair, D. (1982) Alpine metamorphism of diabase dikes in the Oetztal-stubai metamorphic complex. TMPM Tsch. Min. Petr. Mitt. v. 29, p. 205-221.

Ripley, E.M. and Ohmoto, H. (1980) A FORTRAN program for plotting mineral stabilities in the Fe-Cu-S-O system in terms of log (SO_4/H_2S) or log f_{O_2} vs pH or T: Computers Geosci., v. 5, p. 289-300.

Robie, R.A., Hemingway, B.S. and Fisher, J.R. (1978) Thermodynamic properties of minerals and related substances at 298.15K and 1 bar (10^5 pascals) pressure and at higher temperatures. Geol. Surv. Bull., v. 1452, 458p.

Rose, A.W. and Burt, D.M. (1979) Hydrothermal alteration. In: Barnes, H.L. (ed) Geochemistry of Hydrothermal Ore Deposits. New York, Wiley Interscience, p. 173-235.

Shibata, K. and Ishihara, S. (1974) K-Ar ages of major tungsten and molybdenum deposits in Japan. Econ. Geol., v. 69, p. 1207-1214.

Walshe, J.L. and Solomon, M. (1981) An investigation into environment of formation of the volcanic-hosted Mt. Lyell copper deposits using geology, mineralogy, stable isotopes, and a six-component chlorite solid solution model. Econ. Geol., v. 76, p. 246-284.

Taylor, B.E. and Liou, J.G. (1978) The low temperature stability of andradite in C-O-H fluids. Am. Mineral., v. 63, p. 378-393.

Yoon, Y.D. (1984) Petrology of the Intrusive Rocks in the Mt. Taebaek Area. Unpub. Msc. thesis, Kyungpook National University. 60p.

상동 중석 스카른의 생성조건에 관한 연구

문   건   주*

상동 텅그스텐 스카른의 생성온도와 동위원소가 보여준 결과는 광화용액의 근원이 마그마로부터 공급되어진 것으로 추정이 가능해 현 광체 하위부 1km 이내에 화강암류의 존재를 예측케 한바 있다.

스카른 광물군은 중앙의 운모부화대로 부터 측면으로 유체는 이동해 나가면서 평형 조건하에서 형성되어진것 같다. 광물학적 누대는 점차 외곽으로 가면서 시간이 지남에 따라 점차 확대되어 광상전반에 걸쳐 초기 광물군의 잔적을 남기면서 특징적인 스카른을 형성하였다. 중심부의 특징적인 운모-회중석대는 유체의 진화과정의 마지막 단계의 마그마 유체의 성질을 나타내 보이고 있다. 열역학적인 계산에 의한 그림을 이용해 일부 광물의 성분을 단순화시켜 스카른의 생성을 도시함으로써 정량화시켜 생성조건을 표현하였다.

* 動力資源研究所